

## Development of polymeric drug delivery system for recognizing vascular endothelial dysfunction

Kenjiro Ikuta,<sup>a</sup> Takeshi Mori,<sup>a,b,c</sup> Tatsuhiro Yamamoto,<sup>b</sup> Takuro Niidome,<sup>a,b,c</sup>  
Hiroaki Shimokawa<sup>c</sup> and Yoshiki Katayama<sup>a,b,c,d,\*</sup>

<sup>a</sup>Graduate School of Systems Life Sciences, Kyushu University, 744 Motoooka, Nishi-ku, Fukuoka 819-0395, Japan

<sup>b</sup>Department of Applied Chemistry, Faculty of Engineering, Kyushu University, 744 Motoooka, Nishi-ku, Fukuoka 819-0395, Japan

<sup>c</sup>Center for Future Chemistry, Kyushu University, 744 Motoooka, Nishi-ku, Fukuoka 819-0395, Japan

<sup>d</sup>Japan Science and Technology Agency, CREST, 4-1-8 Honmachi, Kawaguchi 332-0012, Japan

<sup>e</sup>Department of Cardiovascular Medicine, Graduate School of Medicine, Tohoku University, 1-1 Seiryomachi, Aoba-ku, Sendai 980-8574, Japan

Received 8 November 2007; revised 3 January 2008; accepted 4 January 2008

Available online 10 January 2008

**Abstract**—The vascular endothelium plays an important role in regulating vascular homeostasis. Damage to the endothelium can lead to cardiovascular diseases such as arteriosclerosis. Therefore, early-stage detection and evaluation of vascular endothelium dysfunction would be very important for effective diagnosis and therapy. We synthesized a polymeric drug carrier bearing an Evans blue analogue as a probing unit for endothelium injury. The polymeric carrier spontaneously formed stable nanoparticles with micelle-like structure in aqueous media and could encapsulate hydrophobic doxorubicin (DOX). The encapsulated DOX showed a sustainable release profile over a period of 10–60 h depending on the loaded DOX concentration. The polymeric carrier specifically adsorbed against the endothelium-injured site in extracted porcine aorta. These properties of the polymeric drug carrier will be suitable for specific drug delivery to endothelium dysfunctional region.

© 2008 Elsevier Ltd. All rights reserved.

### 1. Introduction

The vascular endothelium is a cellular monolayer on the inside blood vessel wall and plays an important role in regulating vascular homeostasis.<sup>1–4</sup> When the endothelium is exposed to free radicals, hypertension, and oxidized low-density lipoprotein (LDL), the endothelium causes inflammation leading to the formation of atherosclerosis. Its earliest changes include endothelial dysfunction such as increasing endothelial permeability, adherence of plasma constituents, and attraction of monocytes.<sup>2</sup> This endothelial dysfunction leads to formation of a fatty streak in atherosclerosis and finally brings about vascular disease such as the spasms in myocardial infarction.<sup>2,4</sup> Therefore, the detection of endothelial dysfunction is important for early diagnosis of and therapy for myocardial disease.

For the diagnosis of and therapy for vascular disease, many studies utilizing such tools as MRI, fluorescence imaging, and drug and gene delivery have been reported.<sup>5–10</sup> In local drug delivery methods, the use of drug- or gene-coated stents provides one of the most promising approaches.<sup>9</sup> These stents are coated with polymers or gels including therapeutic agents. Elutions of these therapeutic agents are controlled by the polymer or gel. This method has primarily been used to prevent restenosis after surgical treatment. Another strategy is active targeting using drug carriers with specific ligands of marker proteins expressed on the cell surface in vascular disease regions. ICAM-1, VCAM-1, and E/P selectin are known to be expressed in dysfunctional endothelium.<sup>11,12</sup> Therefore, drug carriers such as liposome and polymeric micelle modified with ligands<sup>13,14</sup> or antibodies for these adhesion molecules<sup>14–18</sup> and fibrin<sup>19–21</sup> have been widely investigated as targeting tools for vascular diseases.

We have focused on a change of physical properties of the endothelium surface in the early-stages of atherosclerosis.

**Keywords:** Arteriosclerosis; Endothelium dysfunction; Drug delivery systems; Evans blue analogue.

\*Corresponding author. Tel./fax: +81 92 802 2850; e-mail: [ykatatcm@mbbox.nc.kyushu-u.ac.jp](mailto:ykatatcm@mbbox.nc.kyushu-u.ac.jp)

rosis, and found recently that some organic dye molecules can selectively adsorb to an injured endothelium region. In these dyes, Evans blue (EB) shows the most effective discriminating ability. Thus we have recently reported specific MRI imaging of injured carotid artery in rat with newly synthesized EB-based contrast agent, EB-DTPA-Gd.<sup>22,23</sup>

In this report, we describe the synthesis and evaluation of endothelial dysfunction-specific drug carriers using EB analogue (Fig. 1a and b). We synthesized a polymeric carrier, which consisted of a hydrophobic main chain [poly(*N-tert*-butylacrylamide)], hydrophilic graft chain [poly(ethylene glycol)], and EB analogue as a probing unit for vascular disorder. This copolymer is expected to form a micelle-like nanoparticle<sup>24</sup> that has a hydrophobic core of poly(*N-tert*-butylacrylamide) and a hydrophilic outer shell of poly(ethylene glycol). We encapsulated doxorubicin (DOX) in the nanoparticle as an inhibiting drug of smooth muscle cell proliferation.<sup>25</sup> We then characterized the nanoparticle with dy-

namic light scattering and also investigated the targeting ability of the nanoparticle using extracted porcine aorta. Our results showed that the nanoparticle incorporating DOX demonstrates specific adsorption to the injured aorta. Thus, our polymeric drug carrier will potentially be suitable for specific drug delivery to endothelium dysfunctional regions.

## 2. Results and discussion

### 2.1. Loading of DOX in the polymeric carriers

We designed a graft-type polymeric carrier (Fig. 1a and c) in which the hydrophobic main chain was grafted with hydrophilic PEG chains and was modified with a sensing unit for recognizing endothelium dysfunction. This copolymer was synthesized by radical copolymerization with PEG macromonomer, NBAAm, and Boc-AS as a precursor of the EB analogue (Fig. 1c). EB analogue modification was achieved by diazo-coupling of

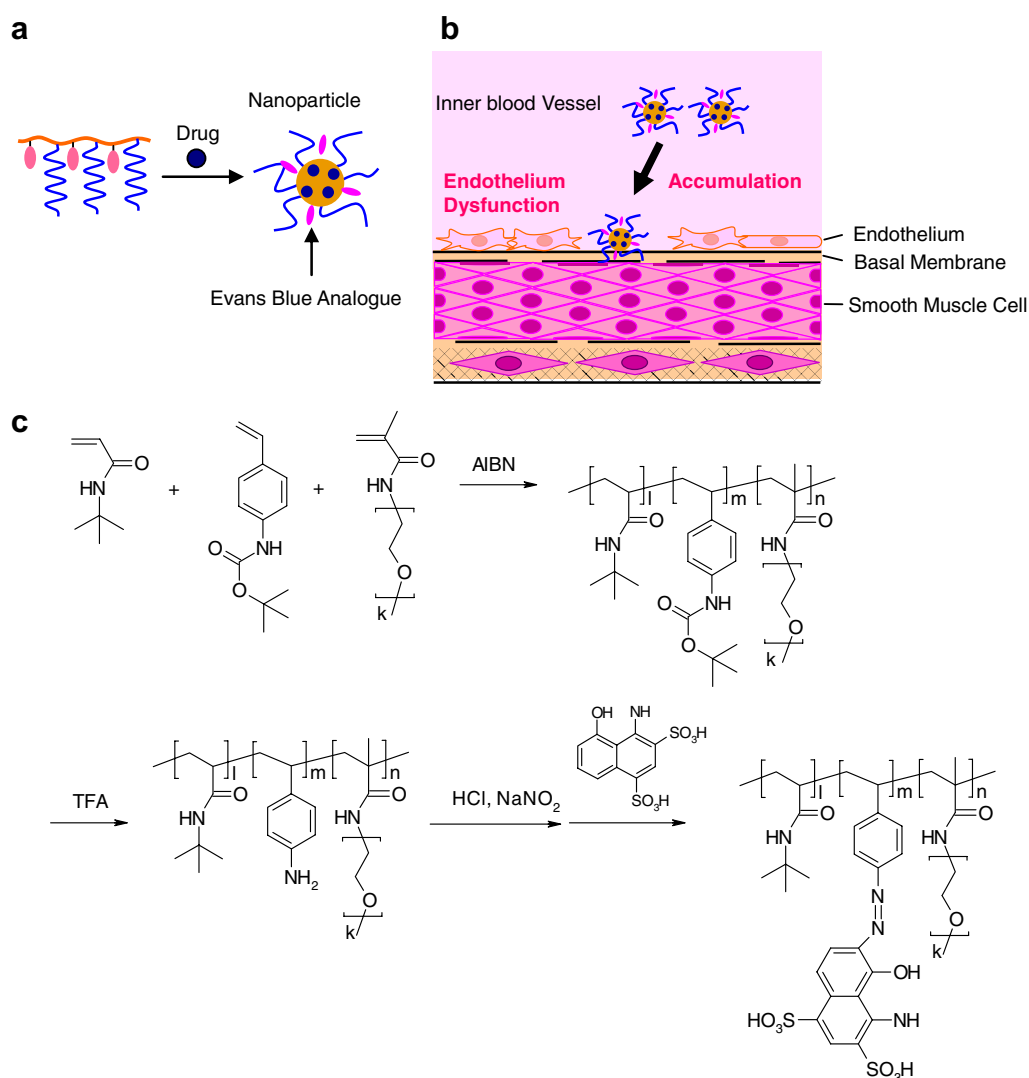


**Figure 1.** (a) Schematic representation of spontaneous formation of drug-loaded polymeric carrier bearing Evans blue analogue, (b) targeting concept of the dye-bearing polymeric carrier to endothelium dysfunction site, and (c) the scheme of synthesis for polymeric carriers.

**Table 1.** Fractions of each monomeric unit in copolymers

Sample code	In feed NBAAm/Boc-AS/PEG (mol/mol/mol)	In copolymer		Conversion (%)
		EB analogue (wt%)	PEG (mol%)	
BEP10-1	89/10/1	3.8	0.3	75.4
BEP10-5	85/10/5	4.2	7.0	54.0
BEP20-5	75/20/5	8.8	4.7	66.7
BEP30-5	65/20/5	5.3	3.5	68.3
BEP0-5	95/0/5	—	2.4	71.8
BEP0-10	90/0/10	—	4.8	42.0

**Table 2.** Molecular weights of copolymers

Sample code	$M_n$	$M_w$	$M_w/M_n$
BEP10-1	18,000	26,800	1.59
BEP10-5	20,400	36,000	1.76
BEP20-5	11,800	44,400	3.76
BEP30-5	16,500	54,000	3.27
BEP0-5	19,600	59,800	3.05
BEP0-10	69,900	408,000	5.84

the copolymer with 1-amino-8-naphthol-2,4-disulfonic acid monosodium salt. The conditions of polymerization and the molecular weights of the obtained polymers are shown in Tables 1 and 2, respectively. When the mole fraction of Boc-AS was increased, the molecular weight distribution of the copolymer became wider (BEP10-5, BEP20-5, BEP30-5). Because of the wide molecular weight distribution, we did not use BEP20-5 and BEP30-5 for DOX loading experiment.

Loading of DOX into the polymeric carrier was achieved by changing the solvent from DMF to deionized water with dialysis, and non-loaded DOX was removed by ultrafiltration. The quantities of loaded DOX in the polymeric carrier (BEP10-5) under various loading conditions are summarized in Table 3. The quantity of loaded DOX in the polymeric carrier increased with increases in the DOX concentrations in the preparation solutions (Run 1–6 and 7–9). In addition, the efficiency of DOX loading (loaded DOX/feed DOX) also improved with increases in the carrier concentration (Run 4/7, 6/9). The maximum loading was 15.9 wt% in Run 9, and the loading efficiency was over 50%. These results indicate that these carriers can load DOX with comparable efficiency to other reported polymeric carriers.<sup>26,27</sup>

**Table 3.** Amount of loaded DOX in BEP10-5 carrier

Run	Polymer (mg/mL)	Feed DOX (mg/mL)	Loaded DOX/polymer (wt%)	Loaded DOX/feed DOX (wt%)
1	0.4	0.06	4.6	31.0
2	0.4	0.1	10.0	39.8
3	0.4	0.2	10.8	21.6
4	0.4	0.3	14.4	19.2
5	0.4	0.4	14.4	14.4
6	0.4	0.6	15.8	10.6
7	2.0	0.3	5.9	39.0
8	2.0	0.5	11.2	44.8
9	2.0	0.6	15.9	53.1

## 2.2. Characterization of polymeric carriers

The polymeric carrier was expected to form micelle-like structure consisting of a hydrophilic PEG shell and a hydrophobic polyNBAAm core in aqueous solution. Therefore, a copolymer with insufficient PEG content would not disperse stably in deionized water after the dialysis. Indeed, BEP10-1, which has the smallest PEG content (0.3 mol%) in the synthesized copolymers, formed large aggregates (average diameter = 1.5  $\mu$ m) due to the low dispersion stability. In contrast, BEP10-5, which contains a large number of PEG chains (7.0 mol%), formed stable small particles with an average diameter of 152 nm. This particle is considered to have consisted of about 25–30 polymer molecules, which were estimated with static light scattering experiment using Zetasizer Nano ZS.

The average size and  $\zeta$ -potential of DOX-loaded polymeric carriers (BEP10-5) are shown in Figure 2a–c. When DOX was encapsulated, the average diameter of the polymeric carrier became smaller than those of non-loaded carriers (Fig. 2a and b). This change was probably due to the increase in the compaction of the hydrophobic core with the hydrophobic interaction between DOX and the EB analogue, because BEP0-5 and BEP0-10 that did not contain EB analogue could not incorporate DOX. The  $\zeta$ -potential of non-loaded polymeric carrier was  $-20$  mV (Fig. 2c). This result is most likely due to the localization of the anionic EB analogue on the surface of the particle. In contrast, the  $\zeta$ -potential approached to neutral with the DOX loading, indicating that anionic EB core of the polymeric carrier was neutralized by the loading of cationic DOX. This interaction between DOX and the EB analogue would be based on the electrostatic as well as the hydrophobic interaction.

Then, the stability of the polymeric carrier was evaluated. The time course of the photon count rate per second and the average size of DOX-loaded polymeric carrier (Table 3, Run 9) in PBS(–) remained constant up to 200 min (Fig. 2d). These results demonstrated the high stability of the polymeric carrier under the physical saline condition due to the hydrophilic PEG shell.

### 2.2.1. Release of DOX from the polymeric carriers.

Determination of the release rate of DOX from the polymeric carriers was carried out by measuring the fluorescence of DOX in the eluting solution during

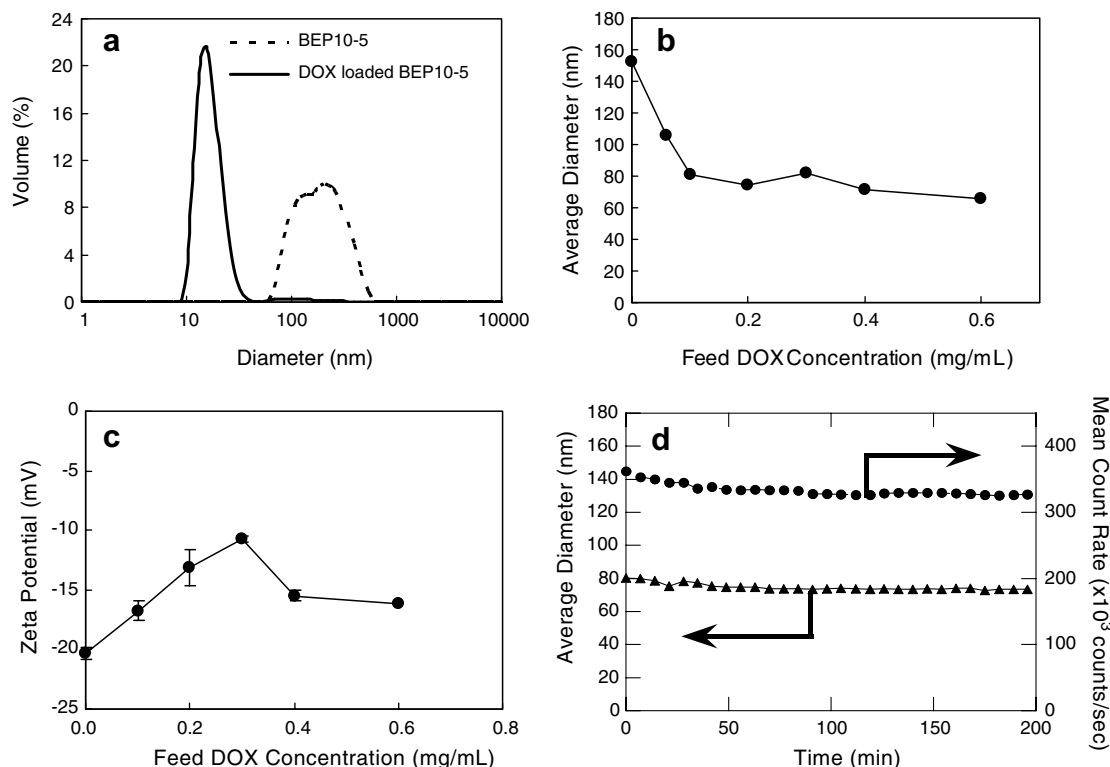


**Figure 2.** Size distribution and  $\zeta$ -potential of the polymeric carriers (1.0 mg/mL) in the presence or absence of DOX. (a) Size distribution of non-loaded and DOX-loaded BEP10-5 (Run 9), (b) average diameter, (c)  $\zeta$ -potential of the polymeric carrier, and (d) time course of the average diameter and the mean count rate of DOX-loaded BEP10-5 (Run 9) after the dissolution in PBS(-).

the dialysis of the carrier dispersion. When 0.6 mg/mL of DOX was used for the loading (Table 3, Run 9), 26% of the loaded DOX was released over a period of 10 h (Fig. 3a, ●). The time course of the DOX release did not have a burst phase which was observed in free DOX (Fig. 3a, ○), suggesting a relatively strong interaction between DOX and the carrier. When the loading DOX concentration was 0.3 mg/mL (Table 3, Run 7), the time course of the DOX release similarly showed no burst phase (Fig. 3b, ●). In both the DOX concentrations, DOX was released gradually over a period of 10–60 h. These sustainable release profiles will be sufficient for successful application as a drug carrier.

### 2.2.2. Evaluation for the adsorption of polymeric carrier to Matrigel-coated and cultured endothelium surfaces.

The basal membrane and extracellular matrix are exposed in the injured endothelial area of vascular surface due to a detachment of endothelium. Since Matrigel consists of component proteins of basal membrane, we used a Matrigel-coated surface as a model of injured endothelial region. The adsorption of the polymeric carrier was evaluated from the decrease of the carrier concentration in supernatant solution after treatment with a Matrigel-coated surface. Matrigel was diluted with medium and was used to coat each well of a 96-well plate. Microscopic images of the gel-coated and cell-coated wells are shown in Figure 4a and b, respectively. The

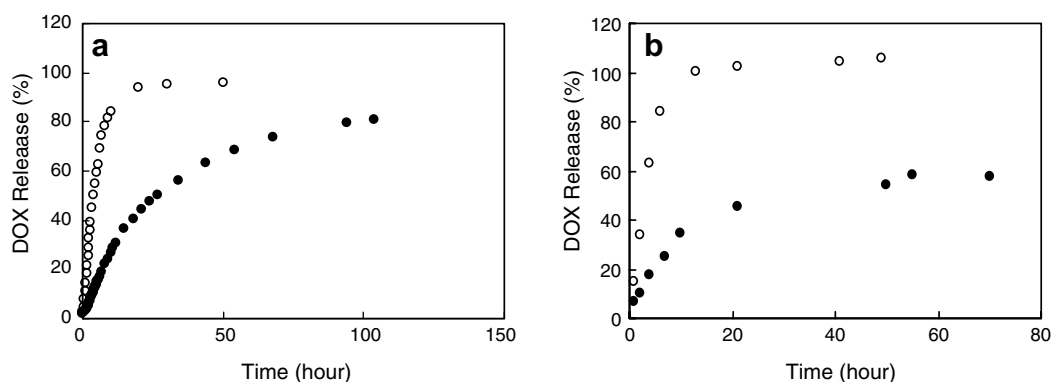


**Figure 3.** Time course of DOX release from the carrier during dialysis. 0.6 mg/mL (a) or 0.3 mg/mL (b) of DOX was used in the nanoparticle preparation. Closed and open circles indicate DOX-loaded carriers and free DOX.

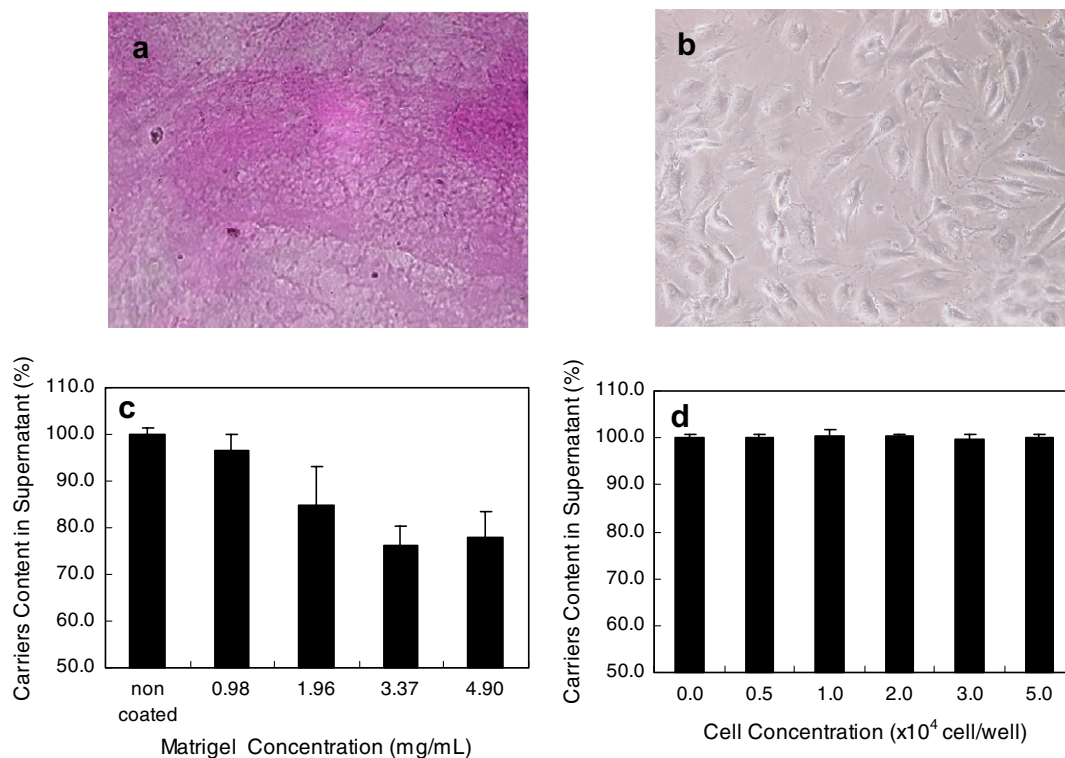


**Figure 4.** Microscopic images of Matrigel-coated (a) or endothelium-coated (b) wells, and changes of the carrier concentrations in supernatant after the treatment with Matrigel-coated (c) or endothelium-coated (d) wells.

reddish violet color resulting from the carrier adsorption was observed clearly in the gel-coated well. The adsorption of the carrier increased with increases in the Matrigel concentration in the coating solution (Fig. 4c). On the other hand, the adsorption of the carrier to endothelial cells was not observed irrespective of the number of cells in the well (5000–50,000 cell/well) (Fig. 4d). These results indicate that the polymeric carrier tended not to adsorb to areas of intact endothelium, but did adsorb to an extracellular proteins in areas of dysfunctional endothelium.

### 2.3. In vitro evaluation of the targeting ability of polymeric carriers against endothelium-injured area

The targeting abilities of the polymeric carrier and drug-loaded carrier were investigated using excised porcine aorta, in which endothelium of half area was injured mechanically. Marked accumulations of the polymeric carrier were observed only in the injured area (Fig. 5a–f). The reddish color became deeper when polymeric carrier concentrations were increased (Fig. 5c and d). DOX concentrations on the aorta slip were compared between injured and intact areas of endothelium. Thus, the same area (1 × 1 cm) of injured or normal regions was taken and lysed. The DOX was then extracted with 2-propanol. As shown in Figure 5g, when the aorta sample was treated with the saline solution of the DOX-loaded carrier, the amount of DOX in the injured area was found to be fourfold greater than that in the intact area. In the case of serum solution, the accumulation of DOX to the injured area was still three times larger. On the other hand, in the case of the

DOX-loaded control carrier poly(benzylmethacrylamide-*co*-PEG), which did not have EB analogue moiety, the adsorption of the carrier to both the injured and intact areas was not observed. These results indicate that the EB analogue modified on the carrier is essential for endothelium-injured sites' recognition. The introduced PEG side chains may suppress the interaction between the EB analogue and endothelium-injured site, due to the steric hindrance. However, the negative value of  $\zeta$ -potential of our particle indicates that the PEG side chains cannot shield the negative charge of the EB analogue units and the particle actually recognized the endothelium injury. Thus, we expect that our polymer may form loose and dynamic complex, which is different from common core-shell type polymer micelle that is seen in block copolymer's micelle. The EB analogue units may be able to appear sometimes on the surface of the particle due to the dynamic motion of the polymer chains. Although the target molecule of the EB analogue recognition has not been clarified yet, the experiment using a Matrigel-coated surface revealed that the EB analogue adsorbs to extracellular matrix. The EB analogue of polymeric carrier may bind to some proteins expressed specifically in the inflammation site because a MRI contrast agent having the same EB analogue unit was also adsorbed in early-stage atherosclerosis in ApoE knockout mice.<sup>28</sup>

### 3. Conclusion

We report here a drug delivery system for vascular endothelial dysfunction using EB analogue as a ligand. The

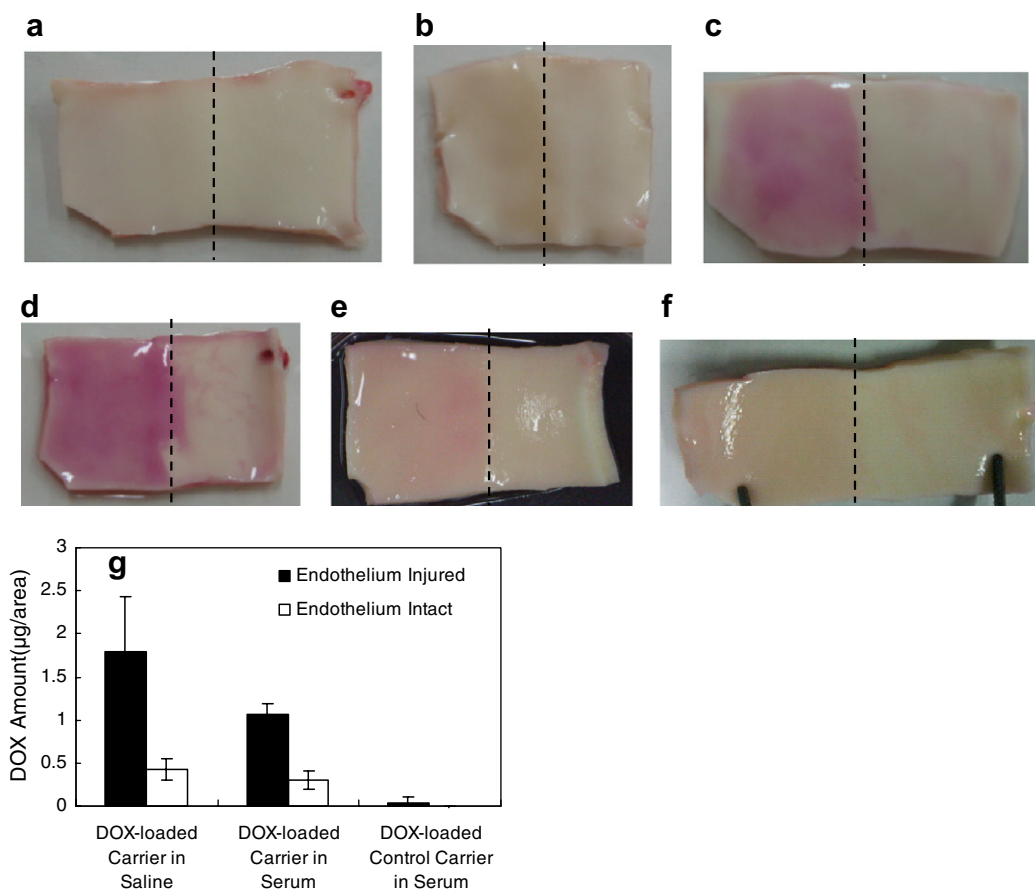


**Figure 5.** Specific adsorption of the polymeric carriers against porcine aorta having injured (left area) and intact regions (right area). Photographs of the opened aorta slips after treatment with the polymeric carriers (a–f). Photoimages after the treatment with saline (a), BEP10-1 (20 mg/mL) (b), BEP10-5 (20 mg/mL) (c), BEP10-5 (40 mg/mL) (d), DOX-loaded BEP10-5 (Run 9) (20 mg/mL in saline) (e), or DOX-loaded BEP10-5 (Run 9) (20 mg/mL in serum) (f). (g) Amounts of DOX in the injured (closed bar) and intact areas (open bar).

synthesized polymeric carrier was found to be capable of encapsulating hydrophobic drug at sufficient concentrations for delivery to an endothelium dysfunction region. In addition, the polymeric carrier was observed to accumulate specifically to the endothelium injured region of the porcine aorta slip. These properties of the polymeric carrier are potentially useful for the development of medical treatment for vascular disease.

## 4. Experimental

### 4.1. Materials

*N*-*tert*-Butylacrylamide (NBAAm), di-*tert*-butyl dicarbonate, sodium nitrite, *N*-acryloxysuccinimide, benzylamine, and DOX were purchased from Wako Pure Chemical Industries, Ltd (Osaka, Japan). 4-Aminostyrene and 1-amino-8-naphthol-2,4-disulfonic acid monosodium salt were from Tokyo Kasei Co., Ltd (Tokyo, Japan). *O*-(2-Aminoethyl)-*O'*-methylpoly-ethylene glycol (NH<sub>2</sub>-PEG, *M*<sub>w</sub> 5000) was purchased from Sigma-Aldrich Japan K.K. (Tokyo, Japan). 2,2'-Azobis-isobutyronitrile (AIBN) was purchased from Nacalai Tesque, Inc. (Kyoto, Japan). Normal human coronary artery

endothelial cell (HCAEC) was purchased from Cambrex (USA). Matrigel was purchased from Becton–Dickinson and Company (NJ, USA). Endothelium Growth Medium was purchased from Takara (Tokyo, Japan).

### 4.2. Synthesis of polymeric carriers

*N*-Boc-4-aminostyrene (Boc-AS) was synthesized from 4-aminostyrene and di-*tert*-butyl dicarbonate according to the literature.<sup>29</sup> *N*-Methacryloyl-PEG was prepared from NH<sub>2</sub>-PEG (*M*<sub>w</sub> 5000) and *N*-methacryloyloxysuccinimide according to the previously reported method.<sup>30</sup> Polymeric carriers were synthesized by radical polymerization of *N*-methacryloyl-PEG macromonomer, NBAAm, and Boc-AS in *N,N*-dimethylformamide (DMF) (total monomer concentration 0.5 M) at 75 °C overnight under a nitrogen atmosphere using AIBN as a radical initiator. The copolymers were purified with GPC (Bio-Beads S-X-1, Bio-Rad Laboratories, Richmond, CA) by using DMF as an eluent. The desired product was dissolved in trifluoroacetic acid for 3 h to deprotect Boc-AS. The reaction solution was neutralized with sodium bicarbonate and desalted with sodium bicarbonate. The solution was lyophilized to yield a pale yellow solid. The deprotected polymer was then dis-

solved in distilled water/THF [1:1 (v/v)] containing hydrochloric acid on an ice bath. Sodium nitrite was added in small portions to the polymer solution, followed by stirring for 30 min to diazotize below 5 °C. The diazonium salt solution was added dropwise to 1-amino-8-naphthol-2,4-disulfonic acid monosodium salt aqueous solution containing sodium bicarbonate on an ice bath and then stirred for 2 h. The reaction mixture was purified with GPC (Sephadex G-50, Amersham Biosciences, Uppsala, Sweden) in distilled water and then lyophilized to yield a reddish violet solid.

A control polymeric carrier poly(benzylmethacrylamide-*co*-PEG), which did not contain EB analogue units and was used for the targeting experiment using extracted porcine aorta, was synthesized as follows. The poly(*N*-acryloxysuccinimide) (polyNAS) was synthesized by radical polymerization of *N*-acryloxysuccinimide in DMF (monomer concentration 1.0 M) at 75 °C overnight under a nitrogen atmosphere using AIBN as a radical initiator. The obtained polymer was purified by reprecipitation with acetone. The polyNAS was reacted with benzylamine and NH<sub>2</sub>-PEG in DMF for 12 h to obtain a desired copolymer. The reaction mixture was purified with ultrafiltration (quantitative molecular weight limit 70 kDa, Apollo, Orbital Biosciences, LLC, MA, USA) and then the copolymer was dissolved in deionized water and lyophilized to yield a pale yellow solid.

The molecular weight of the copolymer was determined by GPC using TSK $\alpha$ -gel 3000 and 4000 (TOSOH Co. Ltd, Tokyo, Japan). GPC was performed using TriSEC 302TDA (Viscotek, TX, USA) with refractive-index, viscosity, and light-scattering detectors at 40 °C. DMF containing 10 mM LiBr was used as an eluting solvent with a flow rate of 0.6 mL/min. The mole fractions of EB analogue and PEG were evaluated with the UV–vis absorbance spectrum (UV-2550, Shimadzu Co. Ltd, Kyoto, Japan) and <sup>1</sup>H NMR (400 Hz, JNM-ECP400, JEOL Ltd, Tokyo, Japan).

### 4.3. Loading of DOX into carriers

Loading of drug into the polymeric carrier was carried out by dialysis. DOX and the polymeric carrier were dissolved in DMF. The solution was dialyzed against deionized water using dialysis bag (molecular weight cut-off 10,000 Spectra/Por 6, Spectrum Laboratories Inc., CA, USA), and the carrier solution was ultrafiltered to exclude non-loaded DOX (quantitative molecular weight limit 10 kDa, Apollo, Orbital Biosciences, LLC, MA, USA) and lyophilized to yield a reddish violet solid.

### 4.4. Size distribution and $\zeta$ -potential measurements

The non-loaded carriers or DOX-loaded carriers were dissolved in distilled water or PBS(–) (1.0 mg/mL), and the samples were filtered with a 0.45- $\mu$ m filter. The hydrodynamic diameter distributions and the  $\zeta$ -potential of non-loaded carriers or DOX-loaded carriers were determined by Zetasizer Nano ZS (Malvern Instru-

ment Ltd, Worcestershire, UK) at 37 °C using a He–Ne laser ( $\lambda = 633$  nm) as a light source.

### 4.5. Quantification of loaded and released DOX

The amounts of loaded drug in polymeric carriers were determined as follows. The polymeric carrier was dissolved in DMF for dissociation and was ultrafiltered. Fluorescence of the DOX in the filtrate was measured with a fluorescence spectrometer (RF-5300PC, Shimadzu Co. Ltd, Kyoto, Japan) ( $\lambda_{\text{ex}} = 485$  nm,  $\lambda_{\text{em}} = 586$  nm).

The amount of DOX released from the polymeric carriers was determined by the fluorescence intensity at 586 nm in the eluent of dialysis against PBS(–) using dialysis tubing (molecular weight cut-off 10,000 Spectra/Por CE, Spectrum Laboratories Inc., CA, USA).

### 4.6. Evaluation of the polymeric carrier adsorption onto Matrigel or cultured endothelium

Matrigel coating was carried out by the thin coat method described as follows. Matrigel (9.8 mg/mL, 100–500  $\mu$ L) was diluted with Dulbecco's modified Eagle's medium (DMEM) (500–900  $\mu$ L) without serum and phenol red. The solution 50  $\mu$ L was dropped into each well of a 96-well microtiter plate and incubated at 37 °C for 2 h. After aspiration of the solution, Matrigel coating plate was washed by DMEM without serum and phenol red. HVAEC were also seeded into each well of a 96-well microtiter plate and incubated with supplement (5% FBS, 0.04% hydrocortisone, 0.4% hFGF-B, 0.1% VEGF, 0.1% R3-IGF-1, 0.1% ascorbic acid, 0.1% hEGF, and 0.1% GA-1000) at 37 °C under a 5% CO<sub>2</sub> atmosphere. After an overnight incubation, the culture medium was exchanged to DMEM without serum and phenol red.

The carrier solution (1.0 mg/mL) was then added to the DMEM without serum and phenol red in the Matrigel coating plate or the HVAEC seeded plate and incubated at 37 °C under a 5% CO<sub>2</sub> for 30 min. Absorbance at 536 nm of the supernatant was measured by UV–vis spectrophotometer (Beckman Coulter, Inc, CA, USA). The phase contrast image was obtained by BZ-8000 (Keyence, Osaka, Japan).

### 4.7. Evaluation of the targeting ability of polymeric carriers

An excised porcine aorta was opened to a flat sheet. Half the area of the slip was then scratched softly to cause endothelium damage. The aorta was dipped into an aqueous solution of the polymeric carrier or serum solution for 60 s and then washed with saline. DOX-loaded poly(benzylmethacrylamide-*co*-PEG) carrier that did not contain EB analogue was used as a control carrier (average hydrodynamic diameter: 83.6 nm). The aorta was cut to 1  $\times$  1 cm<sup>2</sup> and homogenized in acidified 2-propanol (9/1 = 2-propanol/1 M hydrochloric acid).<sup>31</sup> The lysate solutions were allowed to stand at 4 °C for 12 h to extract the drug and then centrifuged at 8000g for

10 min. The fluorescence intensity at 553 nm ( $\lambda_{\text{ex}}$ : 485 nm) in the supernatants was measured.

### Acknowledgment

We thank the Uehara Memorial Foundation for their financial support.

### References and notes

- Ross, R. *Nature* **1993**, *362*, 801–809.
- Ross, R. *N. Engl. J. Med.* **1999**, *340*, 115–126.
- Bazzoni, G.; Estrada, O. M. M.; Dejana, E. *Trends Cardiovasc. Med.* **1999**, *9*, 147–152.
- Fuster, V. *Circulation* **1994**, *90*, 2126–2146.
- Choudhury, R. P.; Fuster, V.; Fayad, Z. A. *Nat. Rev. Drug Discov.* **2004**, *3*, 913–925.
- Wickline, S. A.; Neubauer, A. M.; Winter, P.; Caruthers, S.; Lanza, G. *Arterioscler. Thromb. Vasc. Biol.* **2006**, *26*, 435–441.
- Melo, L. G.; Gnechi, M.; Pachori, A. S.; Kong, D.; Wang, K.; Liu, X.; Pratt, R. E.; Dzau, V. J. *Arterioscler. Thromb. Vasc. Biol.* **2004**, *24*, 1761–1774.
- Hajitou, A.; Pasqualini, R.; Arap, W. *Trends Cardiovasc. Med.* **2006**, *16*, 80–88.
- Gershlick, A. H. *Atherosclerosis* **2002**, *160*, 259–271.
- van Nieuw Amerongen, G. P.; van Hinsbergh, V. W. M. *Vasc. Pharmacol.* **2003**, *39*, 257–272.
- Cybulsky, M. I.; Gimbrone, M. A. *Science* **1991**, *251*, 788–791.
- Nakashima, Y.; Rains, E. W.; Plump, A. S.; Breslow, J. L.; Ross, R. *Arterioscler. Thromb. Vasc. Biol.* **1998**, *18*, 842–851.
- Lestini, B. J.; Sagnella, S. M.; Xu, Z.; Shive, M. S.; Richter, N. J.; Jayaseharan, J.; Case, A. J.; Kottke-Marchant, K.; Anderson, J. M.; Marchant, R. E. *J. Control. Release* **2002**, *78*, 235–247.
- Eniola, A. O.; Hammer, D. A. *Biomaterials* **2005**, *26*, 7136–7144.
- Muro, S.; Dziubla, T.; Qiu, W.; Leferovich, J.; Cui, X.; Berk, E.; Muzykantov, V. R. *J. Pharmacol. Exp. Ther.* **2006**, *317*, 1161–1169.
- Voinea, M.; Manduteanu, I.; Dragomir, E.; Capraru, M.; Simionescu, M. *Pharm. Res.* **2005**, *22*, 1906–1917.
- Blackwell, J. E.; Dagia, N. M.; Dickerson, J. B.; Berg, E. L.; Goetz, D. J. *Ann. Biomed. Eng.* **2001**, *29*, 523–533.
- Asgeirsdottir, S. A.; Kok, R. J.; Everts, M.; Meijer, D. K. F.; Molema, G. *Biochem. Pharmacol.* **2003**, *65*, 1729–1739.
- Thomas, A. C.; Campbell, J. H. *J. Control. Release* **2004**, *100*, 357–377.
- Thomas, A. C.; Campbell, J. H. *Atherosclerosis* **2004**, *176*, 73–81.
- Naik, S. S.; Liang, J.-F.; Park, Y. J.; Lee, W. K.; Yang, V. C. *J. Control. Release* **2005**, *101*, 35–45.
- Yamamoto, T.; Ikuta, K.; Oi, K.; Abe, K.; Uwatoku, T.; Murata, M.; Shigetani, N.; Yoshimitsu, K.; Shimokawa, H.; Katayama, Y. *Anal. Sci.* **2004**, *20*, 5–7.
- Yamamoto, T.; Ikuta, K.; Oi, K.; Abe, K.; Uwatoku, T.; Hyodo, F.; Murata, M.; Shigetani, N.; Yoshimitsu, K.; Shimokawa, H.; Utsumi, H.; Katayama, Y. *Bioorg. Med. Chem. Lett.* **2004**, *14*, 2787–2790.
- Sonoda, T.; Nogami, T.; Oishi, J.; Murata, M.; Niidome, T.; Katayama, Y. *Bioconjug. Chem.* **2005**, *16*, 1542–1546.
- Uwatoku, T.; Shimokawa, H.; Abe, K.; Matsumoto, Y.; Hattori, T.; Oi, K.; Matsuda, T.; Kataoka, K.; Takeshita, A. *Circ. Res.* **2003**, *92*, e62–e69.
- Kataoka, K.; Matsumoto, T.; Yokoyama, M.; Okano, T.; Sakurai, Y.; Fukushima, S.; Okamoto, K.; Kwon, G. S. *J. Control. Release* **2000**, *64*, 143–153.
- Kohori, F.; Yokoyama, M.; Sakai, K.; Okano, T. *J. Control. Release* **2002**, *78*, 155–163.
- Yasuda, S.; Ikuta, K.; Uwatoku, T.; Oi, K.; Abe, K.; Hyodo, F.; Yoshimitsu, K.; Sugimura, K.; Utsumi, H.; Katayama, Y.; Shimokawa, H. *J. Vasc. Res.* **2008**, *45*, 123–128.
- Covolani, V. L.; D'Antone, S.; Ruggeri, G.; Chiellini, E. *Macromolecules* **2000**, *33*, 6685–6692.
- Katayama, Y.; Sonoda, T.; Maeda, M. *Macromolecules* **2001**, *34*, 8569–8573.
- Padilla De Jesus, O. L.; Ihre, H. R.; Gagne, L.; Frechet, J. M. J.; Szaka, F. C., Jr. *Bioconjug. Chem.* **2002**, *13*, 453–461.